A NEW BUTTON-TYPE BEAM POSITION MONITOR FOR BESSY II AND BESSY VSR*

J.-G. Hwang[†], G. Schiwietz[‡], A. Schälicke, M. Ries, V. Dürr, D. Wolk, F. Falkenstern
Helmholtz-Zentrum Berlin für Materialien und Energie GmbH (HZB), Berlin, Germany

Abstract

The implementation of the variable pulse length storage ring upgrade BESSY VSR involves more than one order-of-magnitude differences in the total charge of adjacent short and long bunches within the bunch train. Thus, any signal ringing beyond a nanosecond in time will cause a misreading of beam position and current, specifically for low bunch charges. This calls for an significantly improved performance of the beam-position-monitor (BPM) system for bunch-selective operation. We report on the corresponding design and fabrication of a new button BPM with advanced features, such as impedance matching inside the button as well as optimization of insulator material, button size, and position, for reduced crosstalk between buttons.

INTRODUCTION

There is a strong scientific motivation to generate sub- to picosecond level short X-ray pulses, a timescale on which chemical reactions or phase transitions take place, for investigating the dynamics of fast reactions [1]. The time resolution of experiments in storage rings is typically, however, limited fundamentally in time resolution by the electron bunch length of 30 ~ 100 ps full width at half-maximum (FWHM) apart from several sophisticated methods such as short pulse generation scheme from transversal chipped long bunches [2] and Femtoslicing [1, 3]. The BESSY **V**ariable-pulse-length **S**torage **R**ing (BESSY VSR) project was launched to establish picoseond short pulses for covering the future increasing demands for short X-ray pulses. This is feasible by installing superconducting cavities with resonance frequencies of 1.5 GHz and 1.75 GHz [4] in addition to the fundamental mode 0.5 GHz NC cavities, which generates a beating pattern of the sum voltage, thereby creating alternating buckets for long and short bunches [5]. This provides the capability of user accessible picosecond pulses at a high repetition rate, up to 250 MHz [6]. For a sophisticated operation mode as shown in Fig. 1, in order to preserve the present average brilliance of BESSY II, BESSY VSR has about ten times more beam current in long bunch buckets than short bunch buckets to avoid the longitudinal microwave instability that occurs above a certain threshold current. Due to this disparity in the beam current of long and short bunches, it is particularly difficult to measure the position of the short bunches precisely when there is signal ringing beyond a nanosecond in time [7, 8]. It can cause the

performance deterioration of the bunch-by-bunch feedback system. This stimulates the development of new button-type beam position monitor (BPM).
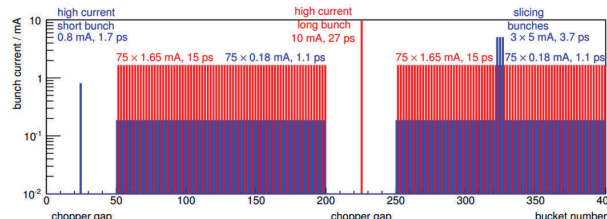

Figure 1: Possible complex filling pattern for BESSY VSR operation with short bunches (blue) and long bunches (red). Trains of low charges short bunches are added to relax beam lifetime and to supply THz power as well as short X-ray pulses at high repetition rate.

LONG-RANGE SIGNAL RINGING

Helmholtz-Zentrum Berlin (HZB) operates the 3rd generation synchrotron radiation facility, BESSY II, since 1999. The BESSY II standard button-type BPMs were developed and installed during construction of the storage ring. We observed a completely different signal shape in the measurements of the BESSY II standard BPM with 1 mA single bunch and multi-bunch train [9]. This can occur because trapped modes inside the insulation of the BPM are not fully damped within 2 ns, which corresponds to the bunch spacing in the storage ring. When the frequency of the trapped mode is a harmonic of the fundamental beam frequency f_{RF} = 500 MHz, the accumulative effect over the multi-bunch train can cause significant distortion of not only the shape of the signal but also the amplitude although the amplitude of the signal ringing is small. The spectrum of measured BPM signal during single-bunch operation is shown in Fig. 2.

In the spectrum of the measured BPM signal, two strong trapped modes are present at the frequencies of 5.2 GHz and 5.5 GHz. To confirm the effect of the long-range signal ringing, the evolution of the signal can be calculated by superimposing the measured single-bunch signal V_{single} with bunch spacing Δt_b which can be expressed as

$$V_{accum}(t) = \sum_n V_{single}(t-n\Delta t_b) \int_{-\infty}^{t-n\Delta t_b} ds\delta(s), \quad (1)$$

By using Eq. (1) with 2 ns equi-spaced and equi-populated without concerning transient beam loading effects, the expected signal shape with a multi-bunch filling is calculated.
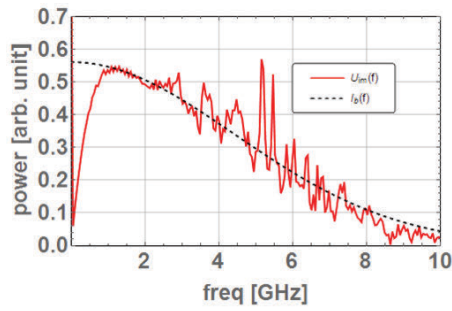
Figure 2: The curve named U_{im} is the Fourier transform of the measured signal and I_b is the spectrum of a Gaussian beam [8].

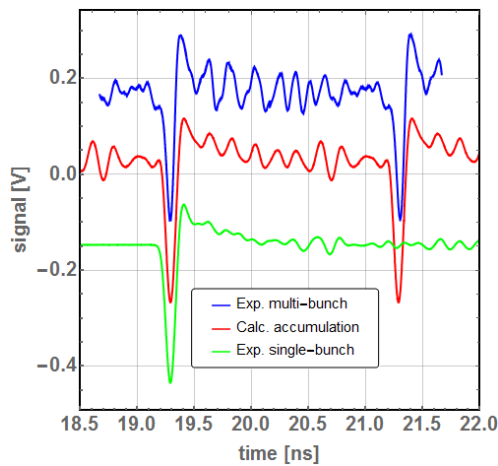It is shown in Fig. 3 with the measured signals with a single bunch and multi-bunch filling.

Figure 3: Measured signals: single bunch (Green) with current of 1 mA, multi-bunch train (Blue) with signal current of 0.8 mA, and the signal calculated (Red) by superimposing the single bunch signal with 2ns spacing.

The long-range signal ringing cause a considerable signal interference to the neighboring bunches. The accumulated signal shows a good agreement in terms of the signal ringing frequency and the local flat-top in front of the second peak. The influence of the long-range signal ringing has proven obviously. To estimate the distortion of the peak value due to the accumulative effects precisely, the relative peak-value spread $\Delta V_{peak}/V_{peak}$ is calculated.

Assuming equivalent bunch charge in the multi-bunch train which represents that the sum of induced voltage on four electrodes Σ_l is a constant, the position of the n-th bunch with the cross-talk coefficient α which represents the strength of the interference to the neighboring bunch is given by

$$x_{n,tot} = x_n + \sum_{l=1}^{n-1} k \frac{\alpha^{n-l}\Delta_l}{(1+\alpha^{n-l})\Sigma_l}, \qquad (2)$$

where x_n is the central position of the n-th bunch, k is the calibration factor, α is the cross talk coefficient, Δ_l and Σ_l are the difference and sum of the l-th bunch signal, respectively.
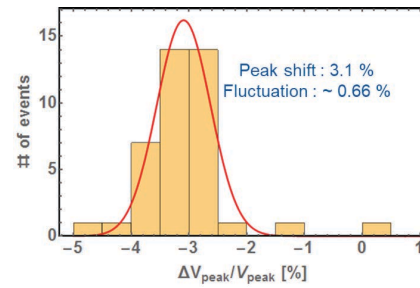

Figure 4: Relative peak-value spread ($\Delta V_{peak}/V_{peak}$) along a multi-bunch train with equivalent bunch charge. With equi-spaced and equi-populated signals, 3% shift and 0.66 % spread of peak values are observed.

From the Eq. (2), the second bunch position is approximately $x_2 \sim x_2 + \alpha x_1$. The peak-value shift due to the signal ringing can cause a 3 % position misreading of the following bunches. In the case of BESSY VSR, this effect causes a severe misreading of the beam position of the short bunches since the filling pattern has a large disparity in the beam current between the short and long bunches.

In order to clarify the source of the long-range signal ringing, the cutoff frequency inside the button is calculated using the physical dimensions and materials. The button structure is a coaxial-type waveguide so that desirable transverse electromagnetic (TEM) mode is allowed to propagate at all frequencies. But at frequencies above the cutoff frequency f_{cut}, the first higher-order mode TE_{11} will also propagate. This higher-order mode defines the cutoff frequency and the TE_{m1}-mode in a coaxial waveguide can be defined as [10]

$$f_{cut} = \frac{1}{\sqrt{\epsilon_r}} \frac{c}{\pi} \frac{m}{r_i + r_o}, \qquad (3)$$

where r_i and r_o are the radii of the inner and outer conductors, respectively, $m = 1, 2, 3, \cdots$, which indicates the field variation in azimuthal direction, and ϵ_r is dielectric constant. Using Eq. (3) and the structure of the BESSY II standard button BPM, the cutoff frequency along the button is calculated and the result is shown in Fig. 5.
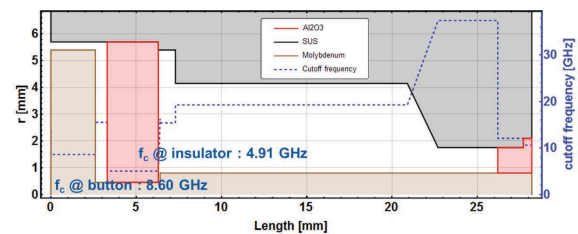

Figure 5: Mechanical structure including material and dimensions and cutoff frequency along the BESSY II standard button BPM with diameter of 11.4 mm, thickness of 2.6 mm, and gap of 0.3 mm

Since the f_{cut} in a coaxial waveguide is inversely proportional to the square root of a dielectric constant of the insulator, the button has a minimum f_{cut} value at the insulator. The BESSY II standard button BPM has the diameter

of 10.8 mm and gap of 0.3 mm. The thickness of the button electrode is 2.6 mm and an aluminum oxide (Al_2O_3) insulator with the diameter of 11.4 mm and thickness of 3 mm was used for a vacuum seal. Therefore, the cutoff frequency at the insulator is 4.91 GHz and it is able to trap long-range modes which are observed in the spectrum of the measured BPM signal as shown in Fig. 2.

NEW BUTTON BPM DEVELOPMENT

For the new button-type BPM, the dimensions of the vacuum chamber are reduced to 55 (H) × 24 (V) mm to improve vacuum conditions near the SRF cavities and to secure the free space of 10 mm between the vacuum chamber and the magnet bore for heating jackets. Furthermore, the diameter of the button is reduced to 8.4 mm to mitigate the coupling between the ports and the effect of trapped modes, and to fit into smaller vacuum chamber dimensions. The clearance gap between the button housing and vacuum chamber is also minimized to avoid the generation of high order modes. The thickness of button is also reduced to 2 mm to enhance the signal intensity by reducing the capacitance of the button. In the right side of the chamber, the synchrotron radiation shade is placed to avoid the power deposited by synchrotron radiation so that the BPM chamber has an asymmetric shape. The cross-section diagram of the new button BPM is shown in Fig. 6.
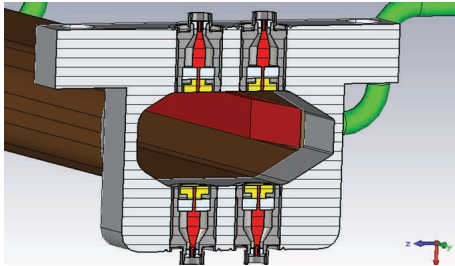

Figure 6: Cross-sectional diagram of new button BPM with diameter of 8.4 mm, thickness of 2 mm, and gap of 0.3 mm.

The new BPM buttons are welded directly on the vacuum chamber without flanges. The insulator materials are evaluated carefully to satisfy a fabrication process and to push the cutoff frequency of the trapped modes higher such that it is damped fully within 0.5 ns. The mode decays in an insulation material proportional to

$$|H(t)| = e^{-\frac{\omega}{2Q}t}, \qquad (4)$$

where $\omega = 2\pi f$ and Q is the quality factor $Q = \epsilon_r'/\epsilon_r''$, where ϵ_r' is the real part of the permittivity and ϵ_r'' is the imaginary part of the permittivity. A fused silica (SiO_2), which has a real part of the permittivity of 3.74 and the imaginary part of the permittivity of 0.00144, is preferred than aluminum oxide Al_2O_3 which has the real part of the permittivity of 9.5 and the imaginary part of the permittivity of 0.00343 because the fused silica has the 44% higher cutoff frequency although the quality factor is 5% smaller than aluminum oxide. The

internal button structure is also optimized to match with the impedance of 50 Ω for reducing TEM-modes reflected back to the chamber. Using Eq. (3) and the structure of the new button BPM, the cutoff frequency along the button is calculated and the result is shown in Fig. 7.
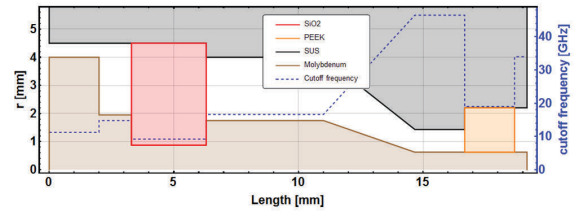

Figure 7: Mechanical structure including material and dimensions and cutoff frequency along the new button BPM.

The cutoff frequency of the trapped mode at the insulator was shifted to a higher frequency by reducing the diameter of the button. In the BESSY II standard button BPM, there are several places where the radius of the outer conductor is changed with a step discontinuity regardless of impedance mismatching. A taper structure is adopted to reduce the reflection between the two different geometries and it is transmission line whose characteristic impedance is gradually tapered from one value to another. The taper is possible to reduce the resulting impedance by providing a tapered region between the two different geometries. As the flexural wave approaches the edge of the taper, the wavenumber progressively increases. For an ideal taper reaching zero thickness, the wavenumber would approach infinity. Therefore, the optimum position of the relative edges between the inner and outer conductor was investigated with geometrical consideration for maintaining the impedance over an inclined plane of the taper.

$$\Delta z_1 = k_{co}\frac{(r_{22}-r_{21})}{z_{pos}}(r_{21}-r_{11}),$$
$$\Delta z_2 = k_{co}\frac{(r_{22}-r_{21})}{z_{pos}}(r_{22}-r_{12}), \qquad (5)$$

where z_{pos} is the taper length, r_{11} and r_{12} are the outer radius of inner and outer conductor at the smaller radius, r_{21} and r_{22} are the outer radius of inner and outer conductor at the larger radius, respectively, and k_{co} is the geometrical coefficient. The reflected pulse as a function of geometrical coefficient k_{co} was calculated.
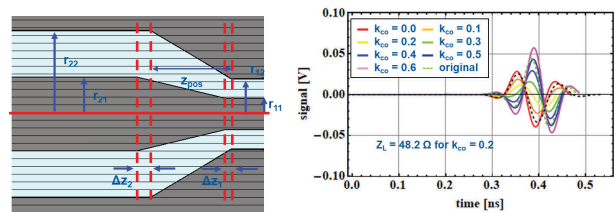

Figure 8: Optimization of two taper edges as function of k_{co} which represents relative position between two conductors.

As shown in Fig. 8, the relative displacement between two conductors can reduce the reflection coefficient from 0.05 to 0.02. Particularly, the taper structure reduces the reflection coefficient significantly compared to the step discontinuity structure which has the reflection coefficient of 0.2. We performed the numerical simulation using CST-PS [11] to confirm the improvement of signal quality by combined effects of the mitigation of trapped resonance modes excited in the insulator and the button lodging hole, and impedance matching.
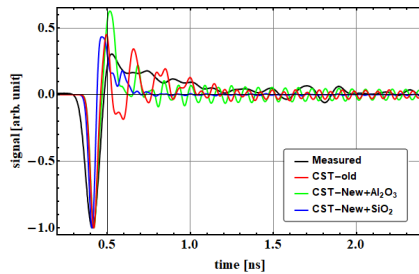

Figure 9: Comparison of signal shape of measured signal from BESSY II standard BPM, CST calculation of BESSY II standard BPM (CST-old), CST calculation of new BPM with aluminum oxide Al_2O_3 and fused silica SiO_2.

As shown in Fig. 9, the new button BPM design with the insulator material of fused silica has relatively short decay-time below 0.3 ns of the signal ringing. However, due to technical difficulties in securing uniformity of the metalization of fused silica surface and subsequent mechanical stability of brazing surface during brazing between fused silica and metal, the insulator material of aluminum oxide is finally determined for the new design. But still there is a glass sealing technique used as feedthroughs in BPMs at PSI and DESY [13, 14] although it is difficult to sustain the impedance matched geometry. The material of the button is determined to be molybdenum, which has an electrical conductivity $\sigma_{MO} = 17 \times 10^6$ S/m, because the power of the trapped more will be predominantly dissipated in the BPM chamber rather than in the well-conducting button [15]. Thus, more than one order magnitude of the power is dissipated on the stainless steel chamber $\sigma_{steel} = 1.3 \times 10^6$ S/m. With the assumption of M equi-spaced and equi-populated bunches [16], the dissipated power by the Wakefield at the new BPM with BESSY VSR operation parameters is 0.42 W which is about 21% lower than the power on present BPM [17].

The long-range trapped resonance modes excited in the insulator and the gap between the electrode and button housing can lead to beam coupling instability [12] so that the longitudinal beam impedance as a function of the frequency is calculated using CST-PS. The calculation has also considered the trapped modes in the button lodging hole, button gap, and insulator material since the amplitude of the trapped resonance modes is relevant to the geometric dimension and the material properties of button, housing, and insulator.
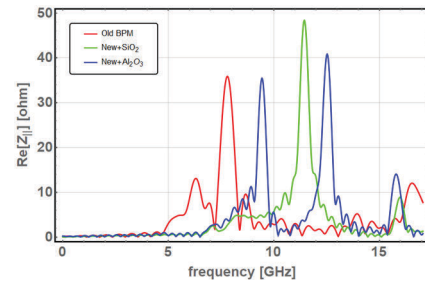

Figure 10: Longitudinal impedance as function of frequency for various BPMs with different insulator materials [18].

As shown in Fig. 10, the button with the insulator material of fused silica has a relatively higher amplitude than the aluminum oxide insulator at relatively higher frequency and the amplitude of the second peak is smaller than the aluminum oxide. The acceptable limit of the narrow-band impedance as a function of the frequency for avoiding coupled-bunch instabilities was estimated using the model in Ref. [19] with the bunch length of 18 ps which corresponds to the nominal bunch length of BESSY II and long bunches of BESSY VSR. The acceptable limit of the narrow-band impedance is relaxed when the resonance frequency of the trapped mode is increased. Since the new button BPM a has peak at relatively higher frequency with a narrow bandwidth, the effect of the narrow-band coupled-bunch instabilities are not crucial.

SUMMARY

In the beam experiment, we observed the signal shape evolution of the BESSY II standard BPM over the multi-bunch train. This indicates signal interference through a long-range signal ringing. We confirmed that the signal ringing causes not only changes of the signal shape over bunch train but also a misreading of the beam position of neighboring bunches in extreme operation modes of BESSY VSR. To mitigate the influence of the signal ringing as well as to reduce wake losses in the new BPM design, the source of long-range signal ringing in the BESSY II standard BPM was investigated and it was found, that certain trapped modes in the aluminum oxide insulator and the button lodging hole are the cause, as these modes have a relatively long decay-time. In the new BPM design, the effects are minimized by optimizing the tapered structure to improve the impedance matching between the two different geometries, reducing the button radius, and by replacing the insulator material. But, due to many technical diffculties, the insulator material of aluminum oxide is finally chosen for the new design instead the more favoured fused silica. The dissipated power by the Wakefield is about 21 % lower than the power on present BPM and the effects of the long-range trapped modes are mitigated by increasing the cutoff frequency.

REFERENCES

[1] S. Khan *et al.*, "Femtosecond Undulator Radiation from Sliced Electron Bunches", in *Phys. Rev. Lett.*, vol. 97, no.

7, p. 074801, Aug. 2006. doi:10.1103/PhysRevLett.97.074801

[2] S. Khan, "Ultrashort Pulses from Synchrotron Radiation Sources", in *Synchrotron Light Sources and Free-Electron Lasers*, E. Jaeschke, S. Khan, J. Schneider, J. Hastings, Eds. Basel: Springer International Publishing, 2016.

[3] K. Holldack *et al.*, "Characterization of laser-electron interaction at the BESSY II femtoslicing source", in *Phys. Rev. ST. Accel. Beams*, vol. 8, no. 4, p. 040704, Apr. 2005. doi:10.1103/PhysRevSTAB.8.040704

[4] A. Jankowiak *et al.*, "The BESSY VSR Project for Short X-Ray Pulse Production", in *Proc. IPAC'16*, Busan, Korea, May 2016, pp. 2833–2836. doi:10.18429/JACoW-IPAC2016-WEPOW009

[5] A. Jankowiak, J. Knobloch *et al.*, "Technical Design Study BESSY VSR", Helmholtz-Zentrum Berlin, 2015, doi:10.5442/R0001.

[6] P. Schnizer *et al.*, "Status of the BESSY VSR Project", in *Proc. IPAC'18*, Vancouver, Canada, Apr.-May 2018, pp. 4138–4141. doi:10.18429/JACoW-IPAC2018-THPMF038

[7] G. Schiwietz, J.-G. Hwang, M. Koopmans, M. Ries, A. Schälicke, "Development of the Electron-Beam Diagnostics for the Future BESSY-VSR Storage Ring", in *J. Phys: Conf. Series*, 1067, 072005 (2018); see references therein.

[8] J. G. Hwang *et al.*, "Recent Progress of Bunch Resolved Beam Diagnostics for BESSY VSR", in *Proc. IBIC'18*, Shanghai, China, Sep. 2018, pp. 379–382. doi:10.18429/JACoW-IBIC2018-WEPA02

[9] J.-G. Hwang, G. Schiwietz, M. Ries, A. Schälicke, V. Dürr, D. Wolk, "New button-type BPM design for BESSY VSR", presented at *the Topical Workshop on Diagnostics for Ultra-Low Emittance Rings*, Oxford, UK, Apr. 2018. https://indico.cern.ch/event/682952/contributions/2952193/attachments/1637738/2613742/TW-DULER2018_final.pdf

[10] A. Blednykh *et al.*, "NSLS-II Storage Ring BPM Button Development", in *Proc. IPAC'15*, Richmond, VA, USA, May 2015, pp. 748–750. doi:10.18429/JACoW-IPAC2015-MOPMN021

[11] CST-MWS website : https://www.cst.com/.

[12] M. Masaki, H. Dewa, T. Fujita, S. Takano, and H. Maesaka, "Design Optimization of Button-Type BPM Electrode for the SPring-8 Upgrade", in *Proc. IBIC'16*, Barcelona, Spain, Sep. 2016, pp. 360–363. doi:10.18429/JACoW-IBIC2016-TUPG18

[13] S. Vilcins and D. Lipka, "Mechanical Design of Cryogenic Vacuum Feedthroughs for X-FEL Button BPMs", in *Proc. 3rd Int. Beam Instrumentation Conf. (IBIC'14)*, Monterey, CA, USA, Sep. 2014, paper TUPF11, pp. 332–336.

[14] S. Vilcins and D. Lipka, "Mechanical Design of Cryogenic Vacuum Feedthroughs for X-FEL Button BPMs", in *Proc. 3rd Int. Beam Instrumentation Conf. (IBIC'14)*, Monterey, CA, USA, Sep. 2014, paper TUPF11, pp. 332–336.

[15] I. Pinayev and A. Blednykh, "Evaluation of Heat Dissipation in the BPM Buttons", in *Proc. PAC'09*, Vancouver, Canada, May 2009, paper TH5RFP014, pp. 3471–3472.

[16] E. Métral, "RF Heating from Wake Losses in Diagnostics Structures", in *Proc. 2nd Int. Beam Instrumentation Conf. (IBIC'13)*, Oxford, UK, Sep. 2013, paper THBL1, pp. 929–935.

[17] A. Schälicke, J.-G. Hwang, G. Schiwietz, M. Ries, V. Dürr, D. Wolk, "Button BPMs @ HZB : BESSY II experiences and BESSY VSR design", presented at *BPM button design and manufacturing workshop*, Oxford, UK, May. 2019. https://www.diamond.ac.uk/Home/Events/2019/BPM-button-design-and-manufacturing-workshop.html

[18] J.-G. Hwang, G. Schiwietz, M. Ries, A. Schälicke, F. Falkenstern, V. Dürr, D. Wolk, "Overview of BPM button design and operational issues: BESSY II & VSR", presented at *Advanced Low Emittance Rings Technology*, Ioannina, Greece, Jul. 2019. https://indico.cern.ch/event/819665/contributions/3494685/attachments/1877375/3091959/ALTER-2019_hwang_final.pdf

[19] C.-K. Ng, T. Weiland, D. Martin, S. Smith, and N. Kurita, "Simulation of PEP-II Beam Position Monitors", in *Proc. PAC'95*, Dallas, TX, USA, May 1995, paper MPQ15, pp. 2485-2487.